第 44 卷 第 4 期/2024 年 2 月/光学学报 研究论文

光学学报

# 谷胱甘肽的类氧化酶 Au@$MnO_2$粒子刻蚀荧光检测方法

肖传豪[1*]，梁慧丽[2]

[1]濮阳职业技术学院，河南大学濮阳工学院，河南 濮阳 457000；

[2]濮阳市中医院检验科，河南 濮阳 457000

**摘要** 设计合成了一种UFO状的具有类氧化酶性质的Au@$MnO_2$纳米粒子。Au@$MnO_2$可催化邻苯二胺(OPD)和氧气反应，生成具有荧光的2，3-二氨基吩嗪(DAP)。加入谷胱甘肽(GSH)后，GSH对$MnO_2$的蚀刻导致纳米粒子的催化能力降低，从而使DAP的荧光强度减弱，可实现对GSH的荧光灵敏检测。在560 nm处的荧光强度与GSH浓度(0.01～10 μmol/L和50～1000 μmol/L)呈良好的线性关系，检测限为0.003 μmol/L。此外，该体系对GSH具有很好的选择性，不受其他离子和氨基酸的干扰。重要的是，该传感器不仅可检测水溶液中的GSH，而且可成功检测血清中的GSH。所提方法具有灵敏度高、抗干扰能力强、操作简单等优点，在生物分析和疾病诊断中具有一定的潜力。

**关键词** 荧光；Au@$MnO_2$纳米粒子；类氧化酶；谷胱甘肽

**中图分类号** O657.7 **文献标志码** A **DOI**：10.3788/AOS231700

## 1 引 言

谷胱甘肽(GSH)是活细胞中含量最多、最重要的生物硫醇抗氧化剂[1-2]。GSH不仅能够直接清除自由基，而且是GSH过氧化物酶系统的重要组成部分，可以抵御自由基和活性氧物质引发的氧化损伤[3]。细胞GSH水平与人体健康息息相关，它与各种疾病的进展有关，如肝脏损伤、衰老、癌症、囊性纤维化、神经退行性疾病等[4-7]。

目前，GSH的检测方法主要有比色法[8]、质谱法[9-10]、色谱法[11-13]、磁共振成像法[14-15]、拉曼光谱法[16]、电化学方法[17]等，已被用于测定生物系统中的GSH。然而，以上检测方法存在灵敏度低、速度慢、选择性差、工艺复杂、实验设备昂贵等缺点。因此，有必要开发一种快速、高灵敏度和特异性的GSH传感器。

本文采用两步法合成了UFO状的核壳型二氧化锰包裹金(Au@$MnO_2$)纳米粒子，利用Au@$MnO_2$的类氧化酶性质催化邻苯二胺(OPD)和$O_2$反应，生成具有荧光特性的2，3-二氨基吩嗪(DAP)；在GSH存在的条件下，GSH刻蚀$MnO_2$会降低Au@$MnO_2$的催化性能，从而导致体系的荧光强度降低，实现了对GSH的检测。本文方法具有灵敏度高、抗干扰能力强、操作简单等优点，可用于实际样品中GSH的检测。

## 2 实验部分

### 2.1 试剂与仪器

氯金酸($HAuCl_4$)、柠檬酸钠($C_6H_5Na_3O_7$)、高锰酸钾($KMnO_4$)、30% 过氧化氢($H_2O_2$)、聚烯丙胺盐酸盐(PAH)、OPD、GSH均购于阿拉丁试剂(上海)有限公司。实验试剂均为分析纯，实验用水为超纯水。

实验使用的仪器主要包括：LF-1504003荧光光谱仪(美国赛默飞公司)；H-7560型透射电子显微镜(日本日立公司)；JSM-7800型扫描电子显微镜(日本日立公司)；实验级超纯水器(美国艾科浦公司)。

### 2.2 纳米金的制备

根据文献[18]，采用柠檬酸钠还原法制备纳米金(AuNPs)：在295 mL煮沸的超纯水中加入0.74 mL氯金酸溶液(浓度为100 mmol/L)并搅拌，随后迅速加入4.5 mL(质量分数为0.5%)柠檬酸三钠溶液，在持续加热下剧烈搅拌15 min，可观察到溶液颜色由灰色变为深红色，最终呈透明酒红色。停止加热，搅拌溶液冷却至室温，以备制备Au@$MnO_2$所用。

### 2.3 核壳型Au@$MnO_2$的制备

参考文献[19]制备核壳型Au@$MnO_2$纳米粒子：将1.5 mL(质量浓度为22 mg/mL)$KMnO_4$溶液和上述制备的AuNPs溶液混合。剧烈搅拌反应5 min后，

**收稿日期**：2023-10-25；**修回日期**：2023-11-23；**录用日期**：2023-11-30；**网络首发日期**：2023-12-12

**基金项目**：河南省科技攻关项目(232102230084)

**通信作者**：*xiaoshihui1@163.com

将 3 mL(25 mg/mL)聚烯丙胺盐酸盐溶液缓慢加入到上述混合物中,搅拌 1 h,可观察到溶液颜色在此过程中由紫色变为黄色,最终呈现深绿色。随后,以 12000 r/min 离心 10 min 除去未参加反应的物质,用超纯水反复洗涤来纯化合成的 $Au@MnO_2$ 纳米粒子。纯化后的 $Au@MnO_2$ 纳米粒子分散于 100 mL 蒸馏水中储存在 4 ℃下备用。

### 2.4 测定方法

首先,将 400 μL 水、300 μL $Au@MnO_2$ 和 100 μL $KH_2PO_4$-$K_2HPO_4$ 缓冲液(0.2 mol/L,pH=7.2)和 100 μL GSH(浓度为 10 nmol/L~1 mmol/L)在常温(25 ℃)下混合反应 15 min。然后,将 100 μL OPD(0.1 mmol/L)分别加入到上述溶液中常温反应 15 min,在紫外灯照射下观察溶液荧光颜色变化并记录荧光发射光谱。

## 3 结果与讨论

### 3.1 检测原理

基于 $Au@MnO_2$-OPD 系统荧光检测 GSH 原理如图 1 所示。具有氧化酶性质的 UFO 状 $Au@MnO_2$ 催化 OPD 和空气中的氧气反应,生成具有荧光的 DAP。当体系中有目标物 GSH 存在时,GSH 会和 $Au@MnO_2$ 纳米粒子的 $MnO_2$ 外壳发生刻蚀反应,导致纳米粒子的氧化酶催化能力减弱,从而导致溶液的荧光减弱,实现对 GSH 的灵敏检测。

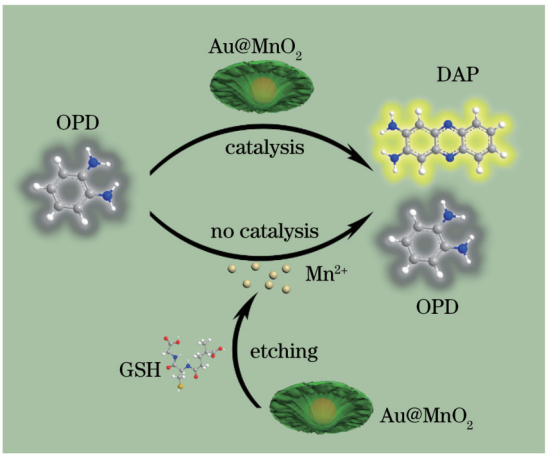


图 1 基于 $Au@MnO_2$-OPD 系统荧光检测 GSH 原理示意图

Fig. 1 Schematic of fluorescence detection of GSH based on $Au@MnO_2$-OPD system

### 3.2 $Au@MnO_2$ 纳米粒子的表征

对所制备的纳米材料进行表征。由图 2(a)、(b)的扫描电子显微镜(SEM)和透射电子显微镜(TEM)图像可知,所得核壳型 $Au@MnO_2$ 纳米粒子呈 UFO 状,直径约为 58.8 nm,分散性良好。图 2(c)所示为纳米粒子的核壳结构。这样的形貌和尺寸使得 $Au@MnO_2$ 纳米粒子作为催化剂时具有较好的催化性能。当 $Au@MnO_2$ 纳米粒子和 GSH 反应时,可以从 TEM 图像[图 2(d)]上清晰地看到纳米金核周围散落的碎片,表明 $Au@MnO_2$ 纳米粒子已被 GSH 刻蚀。

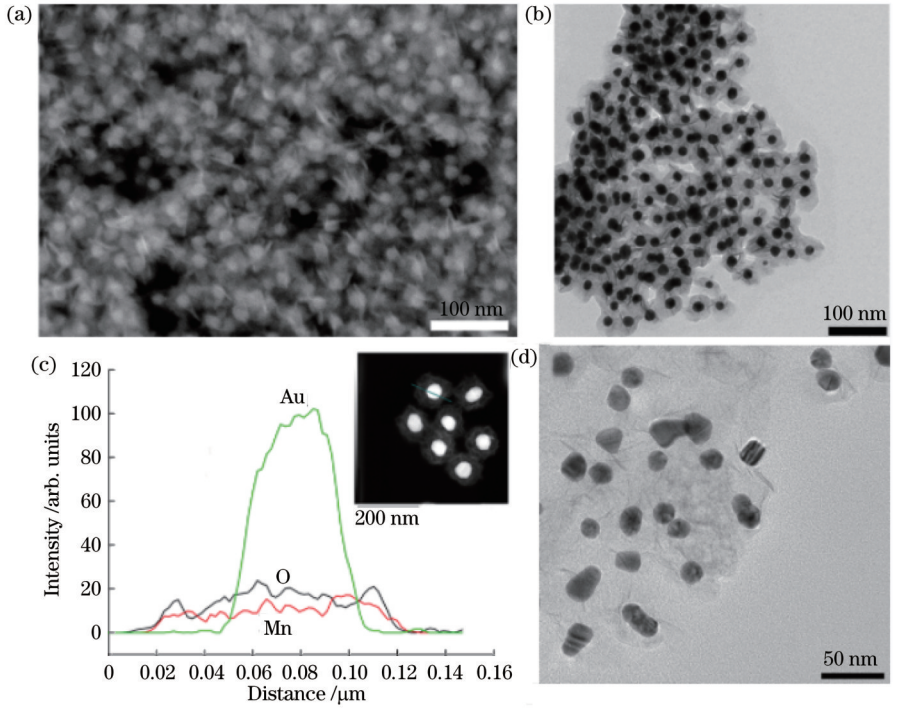


图 2 $Au@MnO_2$ 纳米粒子结构表征。UFO 状 $Au@MnO_2$ 纳米粒子的(a)SEM 图像、(b)TEM 图像、(c)线性扫描图像;(d)被 1 mmol/L GSH 刻蚀后的 $Au@MnO_2$ 纳米粒子 TEM 图像

Fig. 2 Structural characterization of $Au@MnO_2$ nanoparticles. (a) SEM image, (b) TEM image, and (c) linear scanning electron microscopy of UFO shaped $Au@MnO_2$ nanoparticles; (d) TEM image of $Au@MnO_2$ nanoparticles etched by 1 mmol/L GSH

### 3.3 溶液 pH 值对体系荧光强度的影响

本实验选用 0.2 mol/L 的 $KH_2PO_4$-$K_2HPO_4$ 溶液作为缓冲体系，考察了缓冲溶液 pH 值对体系荧光强度的影响。当 pH 在 3.6～7.8 范围内时，不同缓冲溶液 pH 值对荧光强度的影响如图 3 所示。可以看到：当 pH＜7.2 时，荧光强度值随 pH 值的增加而增大；当 pH＞7.2 时，荧光强度开始减小。故本实验选择 $KH_2PO_4$-$K_2HPO_4$ 溶液的最佳反应 pH 值为 7.2。

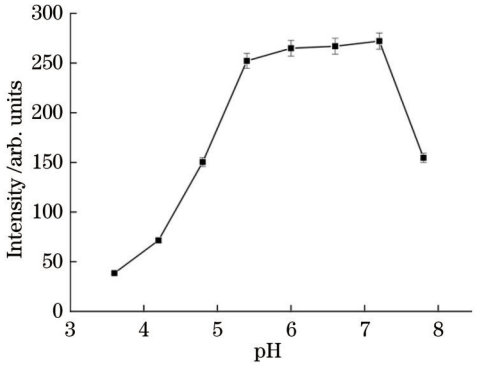


图 3 溶液 pH 值对体系荧光强度的影响

Fig. 3 Effect of solution pH on system fluorescence intensity

### 3.4 OPD 浓度对体系荧光强度的影响

在 pH=7.2 的溶液中，OPD 浓度对体系荧光强度的影响如图 4 所示，随着 OPD 浓度的增加，体系的荧光强度先增大后逐渐减小。当 OPD 浓度为 0.1 mmol/L 时，荧光强度达到最大值，继续增大 OPD 浓度，荧光强度反而降低。因此，实验选择 0.1 mmol/L 作为 OPD 的最优浓度。

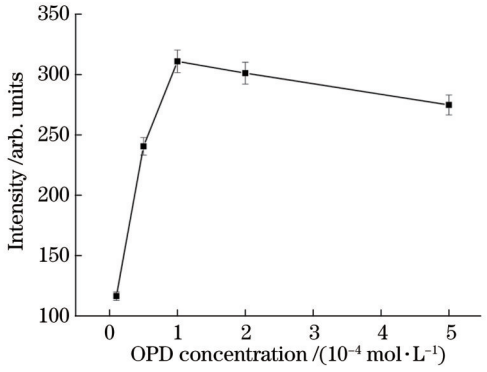


图 4 OPD 浓度对体系荧光强度的影响

Fig. 4 Effect of OPD concentration on system fluorescence intensity

### 3.5 GSH 的孵化时间对体系荧光强度的影响

GSH 的孵化时间对体系荧光强度的影响如图 5 所示，在 0～18 min 范围内每隔 5 min 测定体系的荧光强度，发现体系的荧光强度在 0～15 min 内逐渐减小，随后趋于稳定，故选择 15 min 作为 GSH 的最佳孵化时间。

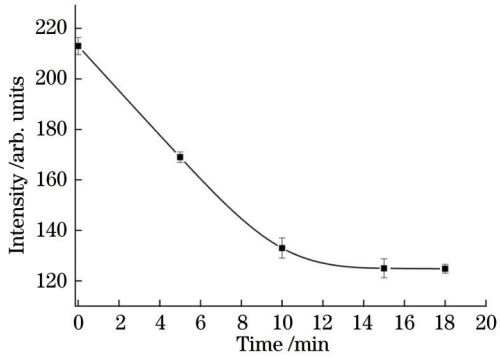


图 5 0.1 mmol/L GSH 的孵化时间对溶液荧光强度的影响

Fig. 5 Effect of incubation time of 0.1 mmol/L GSH on system fluorescence intensity

### 3.6 传感器对 GSH 的荧光响应

为了评估 Au@$MnO_2$-OPD 体系用于 GSH 定量检测的可行性，在最优实验条件下，考察了加入不同浓度（0、10 nmol/L、100 nmol/L、500 nmol/L、1 μmol/L、10 μmol/L、50 μmol/L、0.1 mmol/L、0.5 mmol/L、1 mmol/L）的 GSH 时，560 nm 处体系的荧光峰强度变化（图 6）。如图 6(a)、(b)所示，随着 GSH 浓度的升高，560 nm 处的荧光峰逐渐降低，在紫外灯下溶液颜色由橙色变成黄色再到无色。对 560 nm 处的荧光强度进行拟合分析，结果如图 6(c)所示，荧光强度的变化值（$\Delta F$）与 GSH 浓度的对数值（lg $C$）在 0.01～10 μmol/L 和 50～1000 μmol/L 浓度范围内均呈现良好的线性关系，线性方程分别为 $\Delta F=21.49+11.67\lg C$ 和 $\Delta F=-107.95+144.03\lg C$，相关系数（$R$）分别为 0.99 和 0.98。根据 $3\sigma/S$ 标准计算方法（其中 $S$ 表示线性回归方程的斜率，$\sigma$ 表示 3 个空白样品的标准差），计算出该方法对 GSH 的检测限为 0.003 μmol/L。因此，根据荧光强度变化可实现 GSH 浓度的定量检测。

### 3.7 干扰实验

为探究其他干扰物（金属离子和氨基酸）存在时纳米探针对 GSH 检测的影响，进行了干扰实验，结果如图 7 所示。当向体系中分别加入 5 mmol/L 的氨基酸（酪氨酸、赖氨酸、谷氨酸）以及离子（$Na^+$、$K^+$、$Mg^{2+}$）时，相比于 Au@$MnO_2$-OPD 溶液的荧光强度，所加氨基酸对体系荧光强度的影响很小，但继续向其中加入 0.5 mmol/L GSH 溶液时，荧光强度明显减小，表明该体系对 GSH 具有较好的选择性。

### 3.8 实际样品的检测

为了研究所提方法在实际生物体系中的检测性能，向稀释 50 倍的血清中加入 GSH 标准溶液[所得溶液为磷酸盐缓冲(PBS)溶液]，传感结果如图 8 所示，随着血清样品中 GSH 浓度的增大，溶液的荧光强度逐渐降低，如图 8(a)、(b)所示。560 nm 处体系的荧光强度变化值（$\Delta F$）与 GSH 浓度的对数在 0.01～10 μmol/L

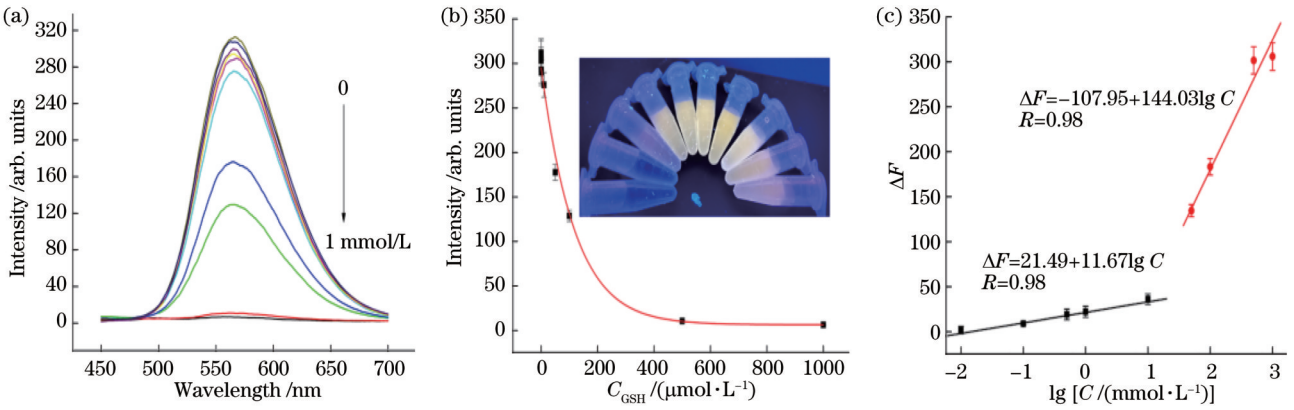


图 6　Au@$MnO_2$-OPD 体系对缓冲溶液中不同浓度 GSH 的传感结果。(a)Au@$MnO_2$-OPD 体系与不同浓度的 GSH 反应前后的荧光光谱;(b)紫外灯下的荧光照片以及荧光强度随 GSH 浓度的变化曲线;(c)荧光信号的变化值与 GSH 浓度对数值的线性关系

Fig. 6　Sensing results of different concentrations of GSH in buffer solution by Au@$MnO_2$-OPD system. (a) Fluorescence spectra of Au@$MnO_2$-OPD system before and after reaction with different concentrations of GSH; (b) fluorescence photos under ultraviolet light and curve of fluorescence intensity changing with GSH concentration; (c) linear relationship between change value of fluorescence signal and logarithmic value of GSH concentration

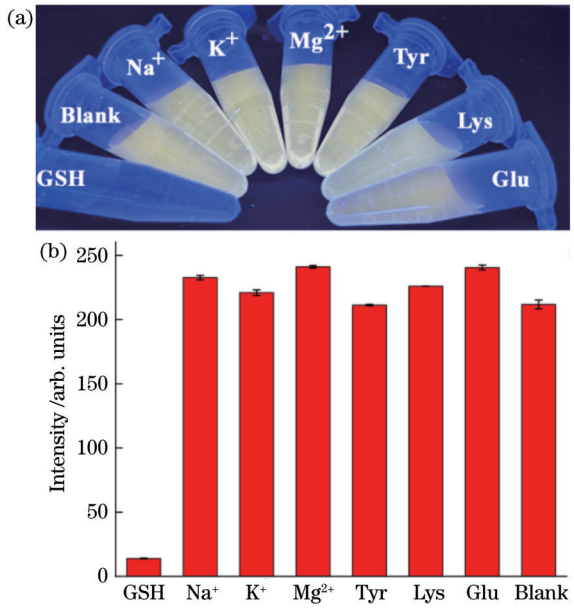


图 7　干扰性实验探究。Au@$MnO_2$-OPD 体系对 5 mmol/L 干扰物(氨基酸和金属离子)和 0.5 mmol/L GSH 的(a)颜色照片和(b)荧光强度柱状图

Fig. 7　Exploration of interference experiments. (a) Color photos and (b) fluorescence intensity histogram of Au@$MnO_2$-OPD system for 5 mmol/L interfering substances (amino acids and metal ions) and 0.5 mmol/L GSH

和 50～1000 μmol/L 范围内均呈良好的线性关系,线性方程分别为 $\Delta F=12.71+4.81\lg C$ 和 $\Delta F=-110.99+109.82\lg C$,相关系数($R$)为 0.99 和 0.95,见图 8(c),结果表明所提方法具有较好的相关性。从缓冲溶液和血清中不同浓度的 GSH 引起的荧光强度对比曲线[图 8(d)]可以看到:当 GSH 浓度很低时,两种溶液中相同浓度的 GSH 引起的荧光强度差异较大;随着 GSH 浓度达到 0.5 mmol/L,荧光强度差异逐渐缩小,表明血清内的其他物质不可避免地造成干扰,但是从血清中不同浓度 GSH 引起的荧光强度趋势来看,结果还是令人满意的。另外,对于同一个血清样品的测试结果,将所提方法的测试结果与作为参考标准的医用紫外酶法的结果进行比较,如表 1 所示。所提方法与紫外酶法在测定血清中的 GSH 含量方面具有高度一致性,说明所提方法可以应用于血清中 GSH 的检测,在临床诊断中具有很好的应用前景。

## 4　结　　论

提出一种简单、快速制备具有类似氧化酶性质的 UFO 状 Au@$MnO_2$ 纳米粒子的方法。基于该材料的氧化酶催化性能,设计了一种快速、简便且灵敏度高的 GSH 荧光检测方法,该方法在 0.01～10 μmol/L 和 50～1000 μmol/L 的 GSH 浓度内呈现良好的线性范围,检测限为 0.003 μmol/L。所提分析方法具有高选择性、高灵敏度、操作简单、检测时间短,在 GSH 的检

表 1　血清样品中的 GSH 检测结果

Table 1　Detection results of GSH in serum samples

| Sample | GSH concentrion /(mmol•L⁻¹) | Detection concentration[a] /(mmol•L⁻¹) | | Recovery /% |
|---|---|---|---|---|
| | | Ultraviolet enzyme method | This method | |
| 1 | 0.58 | 0.57±0.01 | 0.56±0.03 | 96.55 |
| 2 | 0.92 | 0.91±0.06 | 0.90±0.05 | 97.83 |

Note: [a] mean±standard deviation of three determinations.

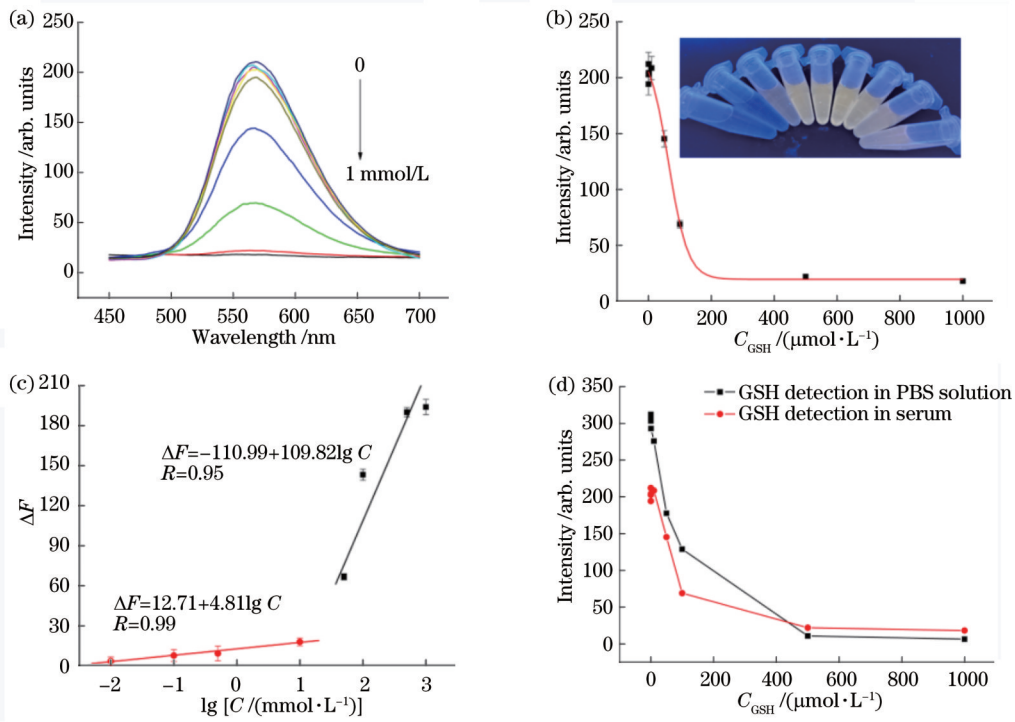


图 8　Au@$MnO_2$-OPD 体系对血清样品中不同浓度 GSH 的传感结果。(a)Au@$MnO_2$-OPD-血清体系与加标不同浓度(0、10 nmol/L、100 nmol/L、500 nmol/L、10 μmol/L、50 μmol/L、0.1 mmol/L、0.5 mmol/L、1 mmol/L)的 GSH 反应前后的荧光光谱;(b)紫外灯下的荧光照片以及荧光强度随血清中 GSH 浓度的变化曲线;(c)荧光信号的变化值与血清中 GSH 浓度对数值的线性关系;(d)在 PBS 溶液和血清中的不同浓度的 GSH 引起的荧光强度对比

Fig. 8　Sensing results of different concentrations of GSH in serum samples by Au@$MnO_2$-OPD system. (a) Fluorescence spectra of Au@$MnO_2$-OPD-serum system before and after the reaction with different concentrations of spiked GSH with different concentrations (0, 10 nmol/L, 100 nmol/L, 500 nmol/L, 10 μmol/L, 50 μmol/L, 0.1 mmol/L, 0.5 mmol/L, 1 mmol/L); (b) fluorescence photos under ultraviolet light and variation curve of fluorescence intensity with GSH concentration in serum; (c) linear relationship between the change value of fluorescence signal and logarithmic value of GSH concentration in serum; (d) comparison of fluorescence intensity caused by different concentrations of GSH in PBS solution and serum

测方面具有较为广阔的应用前景。

## 参　考　文　献


[1] 刘振平, 姜容, 庞钶靖. 还原型谷胱甘肽修饰的金纳米团簇荧光传感器对铜离子的高灵敏检测[J]. 激光与光电子学进展, 2021, 58(14): 1404002.
Liu Z P, Jiang R, Pang K J. Highly sensitive detection of copper ions by reduced glutathione modified gold nanocluster fluorescence sensor[J]. Laser & Optoelectronics Progress, 2021, 58(14): 1404002.

[2] Sedlák J, Hanus L. Changes of glutathione and protein bound SH-groups concentration in rat adrenals under acute and repeated stress[J]. Endocrinologia Experimentalis, 1982, 16(2): 103-109.

[3] Dickinson D A, Forman H J. Cellular glutathione and thiols metabolism[J]. Biochemical Pharmacology, 2002, 64(5/6): 1019-1026.

[4] Hwang C, Sinskey A J, Lodish H F. Oxidized redox state of glutathione in the endoplasmic reticulum[J]. Science, 1992, 257(5076): 1496-1502.

[5] Herzenberg L A, De Rosa S C, Dubs J G, et al. Glutathione deficiency is associated with impaired survival in HIV disease[J]. Proceedings of the National Academy of Sciences of the United States of America, 1997, 94(5): 1967-1972.

[6] Kennedy L, Sandhu J K, Harper M E, et al. Role of glutathione in cancer: from mechanisms to therapies[J]. Biomolecules, 2020, 10(10): 1429.

[7] 许康, 张甜, 邵进军, 等. 谷胱甘肽响应型肿瘤治疗光敏剂的研究进展[J]. 中国激光, 2023, 50(3): 0307202.
Xu K, Zhang T, Shao J J, et al. Progress of glutathione-responsive photosensitizers for tumor therapy[J]. Chinese Journal of Lasers, 2023, 50(3): 0307202.

[8] Han L, Liu S G, Liang J Y, et al. Free-label dual-signal responsive optical sensor by combining resonance Rayleigh scattering and colorimetry for sensitive detection of glutathione based on ultrathin $MnO_2$ nanoflakes[J]. Sensors and Actuators B, 2019, 288: 195-201.

[9] Guo L M, Xiao C S, Wang S, et al. Quantitation of glutathione by quinoline-5, 8-dione-based tag strategy using MALDI mass spectrometry[J]. Journal of the American Society for Mass Spectrometry, 2019, 30(4): 625-633.

[10] Shen B Y, Chen C, Hu K R, et al. Activated charcoal significantly improved the reliability of methods for quantitative analysis of endogenous substances in biological specimens: glutathione and cysteine as cases[J]. Journal of Chromatography B, 2018, 1095: 241-250.

[11] Bollenbach A, Tsikas D. Measurement of the tripeptides glutathione and ophthalmic acid by gas chromatography-mass spectrometry[J]. Analytical Biochemistry, 2022, 644: 113841.

[12] Janeš L, Lisjak K, Vanzo A. Determination of glutathione content in grape juice and wine by high-performance liquid chromatography with fluorescence detection[J]. Analytica Chimica Acta, 2010, 674(2): 239-242.

[13] Szarka A. Quantitative data on the contribution of GSH and

Complex Ⅱ dependent ascorbate recycling in plant mitochondria [J]. Acta Physiologiae Plantarum, 2013, 35(11): 3245-3250.
[14] Rhieu S Y, Urbas A A, Lippa K A, et al. Quantitative measurements of glutathione in yeast cell lysate using $^{1}$H NMR [J]. Analytical and Bioanalytical Chemistry, 2013, 405(14): 4963-4968.
[15] Zhang P S, Zeng J F, Li Y Y, et al. Quantitative mapping of glutathione within intracranial tumors through interlocked MRI signals of a responsive nanoprobe[J]. Angewandte Chemie (International Ed. in English), 2021, 60(15): 8130-8138.
[16] Li Y L, Jiang L, Zou Y Q, et al. Highly reproducible SERS sensor based on self-assembled Au nanocubic monolayer film for sensitive and quantitative detection of glutathione[J]. Applied Surface Science, 2021, 540: 148381.
[17] Yu Arbenin A, Zemtsova E G, Ermakov S S, et al. Three-component working electrode micron-sized Ag particles/$TiO_2$ layer/Ti: template electrochemical synthesis and potential use as electrochemical sensor for glutathione detection[J]. Materials Research Express, 2020, 7(3): 035401.
[18] Grabar K C, Freeman R G, Hommer M B, et al. Preparation and characterization of Au colloid monolayers[J]. Analytical Chemistry, 1995, 67(4): 735-743.
[19] Zhang C, Liu X Z, Xu Z W, et al. Multichannel stimulus-responsive nanoprobes for $H_2O_2$ sensing in diverse biological milieus[J]. Analytical Chemistry, 2020, 92(18): 12639-12646.

# Oxidase-Like Au@$MnO_2$ Particle Etching Triggered by Glutathione for Fluorescence Detection of Glutathione

Xiao Chuanhao[1*], Liang Huili[2]

[1]*Puyang Vocational and Technical College, Puyang Institute of Technology of Henan University, Puyang* 457000, *Henan, China*;

[2]*Department of Clinical Laboratory, Chinese Medicine Hospital of Puyang, Puyang* 457000, *Henan, China*

## Abstract

**Objective** Glutathione (GSH) is the most abundant and important biological thiol antioxidant in living cells. It is not only able to directly scavenge free radicals but also is an important component of the glutathione peroxidase system to resist oxidative damage caused by free radicals and reactive oxygen species. Abnormal cellular GSH levels are considered an important biomarker for human health and are associated with the progression of various diseases, such as liver injury, aging, cancer, cystic fibrosis, and neurodegenerative diseases. Therefore, there is an urgent need to develop a simple method to detect GSH concentration. At present, the main detection methods for GSH include colorimetry, mass spectrometry, chromatography, magnetic resonance imaging, Raman spectroscopy, and electrochemical methods, which have been employed to determine glutathione in biological systems. However, some of the above methods have drawbacks such as low sensitivity, slow speed, poor selectivity, complex process, and expensive experimental equipment. Therefore, a fast, highly sensitive, and specific GSH sensor should be developed.

**Methods** We adopt a two-step method to synthesize UFO-shaped oxidase-like Au@$MnO_2$ nanoparticles (NPs). Firstly, sodium citrate reacts with chloroauric acid to generate AuNPs, and then the $KMnO_4$ solution reacts with polyamine hydrochloride solution to form $MnO_2$ wrapped on the surface of the AuNPs. Then, TEM, SEM, and linear scanning are adopted to characterize the prepared Au@$MnO_2$ nanomaterials. Next, we optimize the reaction parameters of the sensor, such as pH value, OPD concentration, and incubation time of GSH. For GSH sensing, Au@$MnO_2$ catalyzes the reaction of o-phenylenediamine (OPD) with oxygen to produce 2, 3-diaminophenazine (DAP) with fluorescence. The etching of GSH to $MnO_2$ results in weakened catalytic ability of the Au@$MnO_2$ nanoparticles after the addition of GSH, and therefore the fluorescence intensity of DAP exhibits an obvious decrease and realizes the fluorescence sensitive detection of GSH.

**Results and Discussions** In the optimal experimental conditions, the fluorescence peak intensity changes of the system solution at 560 nm are investigated when different concentrations of GSH are added (Fig. 6). As shown in Figs. 6(a) and 6(b), as the concentration of GSH increases, the fluorescence peak at 560 nm gradually decreases. The solution color changes from orange to yellow and then to colorless under ultraviolet light. The fluorescence intensity at 560 nm is fitted and analyzed, as shown in Fig. 6 (c), and a good linear relationship between the fluorescence intensity change at 560 nm and the logarithm of GSH concentration (0.01–10 μmol/L and 50–1000 μmol/L) is acquired with the low detection limit of 0.003 μmol/L. Therefore, quantitative detection of GSH concentration can be achieved based on fluorescence changes. To investigate the influence of the nanoprobe on GSH detection in the presence of other interfering substances (metal ions and amino acids), we conduct interference experiments. The results are shown in Fig. 7. When 5 mmol/L amino acids (tyrosine, lysine, and glutamic acid) and ions ($Na^+$, $K^+$, and $Mg^{2+}$) are added to the system, compared to the fluorescence

intensity of Au@$MnO_2$-OPD, the added amino acids have little effect on the fluorescence intensity of the system. However, when 0.5 mmol/L GSH is further added to the solution, the fluorescence intensity significantly decreases. This indicates that the system has good selectivity for GSH. To study the detection performance of this method in actual biological systems, we employ this sensor to detect GSH in serum. As shown in Fig. 8, the splendid linear relationship between the fluorescence intensity change at 560 nm and the logarithm of GSH concentration (0.01–10 μmol/L and 50–1000 μmol/L) is obtained. Additionally, for the test results of the same serum sample, our method is compared with the medical ultraviolet enzyme method as a reference standard. As shown in Table 1, this method has high consistency with ultraviolet enzyme method in determining GSH content in serum. This method can be utilized for GSH detection in serum and has great application prospects in clinical diagnosis.

**Conclusions** We propose a simple and rapid method for preparing UFO-shaped oxidase-like Au@$MnO_2$ nanoparticles. Based on the oxidase catalytic performance of this material, a fast, simple, and highly sensitive method for fluorescence detection of GSH is designed, which can detect GSH at concentrations of 0.01–10 μmol/L and 50–1000 μmol/L with a detection limit of 0.003 μmol/L. This analytical method has high selectivity, high sensitivity, simple operation, and short detection time, with broad application prospects in GSH detection.

**Key words** fluorescence; Au@$MnO_2$ nanoparticles; oxidase-like; glutathione